Evaluation of time-resolved autofluorescence images of the ocular fundus

Dietrich Schweitzer[1], Martin Hammer[1], Frank Schweitzer[1], Stefan Schenke[1], Elizabeth R.Gaillard[2]

[1]Experimental Ophthalmology, University of Jena, Bachstr. 18, D-07743 Germany,
[2]Dept. of Chemistry/Biochemistry Northern Illinois University, Normal Road/Faraday Hall 324, DeKalb, Il 60115, USA

ABSTRACT

Changes in the metabolism can be assumed as a first sign of several ocular diseases. If such metabolic alterations are detectable, diseases might be treatable, before morphological alterations are manifest. The redox pairs of co-enzymes fluoresce after excitation and change their fluorescence properties depending on the oxidative state of cellular metabolism. Metabolic by-products and connective tissue exhibit also auto-fluorescence. The detection and discrimination of endogenous fluorophores at the fundus by selected excitation or evaluation of emission spectra is not possible with a high spatial resolution. The lifetime of electrons in the excited stage is also substance specific and is not influenced by the absorption spectra of non-fluorescent substances at the fundus. For that reason, a Laser Scanning Ophthalmoscope was developed for the 2-dimensional measurement of time – resolved auto-fluorescence at the living human eye-ground. In first studies, different changes in auto-fluorescence were found after respiration of oxygen between fundus sites. Between young and older persons as well as patients suffering from age-related macular degeneration different lifetime-ranges were detected from the same anatomical region. For comparison, lifetime measurements were performed on single substances. In a first step of interpretation, the frequency distribution of each lifetime in a region of interest can be compared between in vivo and in vitro measurements. Presenting the results in Tau 1-Tau 2 diagrams, specific clusters can be found in both types of measurement, covering each other partially and allowing interpretation of measurements from the living human eye.

Keywords: Lifetime, fluorescence, Laser Scanning Ophthalmoscope, ocular fundus, age-related macular degeneration, Lipofuscin, advanced glycation end-product, NADH, FAD

1.INTRODUCTION

Metabolic alterations are assumed as first sign of some important eye diseases like age-related macular degeneration, diabetic retinopathy, or glaucoma. If it would be possible to detect such changes e.g. in the equilibrium of redox pairs of co-enzymes like nicotinamid-adenindinucleotide (NADH-NAD), of flavin-adenindinucleotide (FADH-FAD) or in the accumulation of metabolic end-products like lipofuscin or advanced metabolic end – products (AGE), diseases might be treatable, before morphological alterations are manifest. The redox pairs of co-enzymes fluoresce after excitation and change their fluorescence properties depending on the oxidative state of cellular metabolism[1]. Metabolic by-products and connective tissue exhibit also autofluorescence[2]. As especially the redox-pairs of co-enzymes characterise the state of metabolism in mitochondria, the investigation of the metabolism at cellular level might be possible as a completely new diagnostic tool in ophthalmology.

The detection and discrimination of endogenous fluorophores at the fundus by selected excitation or evaluation of emission spectra is not possible with a high spatial resolution. The transmission of the ocular media allows measurements at the eye-ground only on the spectral range between 400 nm and about 900 nm. Especially the absorption of the crystalline lens at 400 nm, hinders any specific excitation of endogenous substances at the eye-ground in the short-wave region. On the other hand, the evaluation of emission spectra requires a sufficient high spectrally resolved fluorescence signal, which can practically not be realised with a high spatial resolution. The eye is the receptive organ for light and the maximal permissible exposure[4] is determined so low, that the measuring light causes no damage under all circumstances. So, the maximal permissible exposure of the eye limits the radiation power and the exposition time. Furthermore absorbing fundus substances like xanthophyll influence the spectral characteristics of the

detectable emission spectrum. The spectral reflection of the fundus is between 1 and 10 %. Assuming a diffuse reflection, only about 1% of the entire reflected light is detectable through the pupil of the eye. The auto-fluorescence signal is 2-3 orders weaker than the reflected light. So, about 10^{-6} of the incoming maximal permissible power is detectable as fluorescence signal.
A third way for discrimination of endogenous fluorophores is the measurement of the decay of fluorescence. Principles for detection of dynamic fluorescence and for lifetime calculating are explained in Lakowicz[4]. As shown by Schweitzer[5], the very weak fluorescence signal originating from the eye - ground fulfils optimally the conditions, required for the application of the time-correlated single photon counting. First measurements of the time-resolved auto-fluorescence of the living human eye – ground and of fundus specimen are described by Schweitzer et al.[5,6,7].

2. Technical Arrangement

Based on the experiences with the experimental set – up, described by Schweitzer[5,6] a prototype of a laser scanner ophthalmoscope was developed, permitted for clinical applications. There are some improvements in comparison with the earlier described set – up. Most important for practical application is the use of the laser diode LDH 440 (Picoquant, Berlin, Germany) instead of the mode – locked Ar^+ - Laser ILA 190. This diode emits pulses of about 100 ps FWHM with a maximal repetition rate of 40 MHz. The laser radiation is focused by a collimator in a 10 µm fibre and led in a cLSO – head (Carl Zeiss, Oberkochen, Germany). The mean radiation power in the cornea plane is 60 µW. The power can be increased, but this results in a change of the shape of the excitation pulse. The applied exposition is less than 1% of the maximal permissible exposure[3], also in the worst case. Fig. 1 shows the block diagram of the laser scanner ophthalmoscope for 2-dimensional measurement of time-resolved autofluorescence of the human eye – ground.

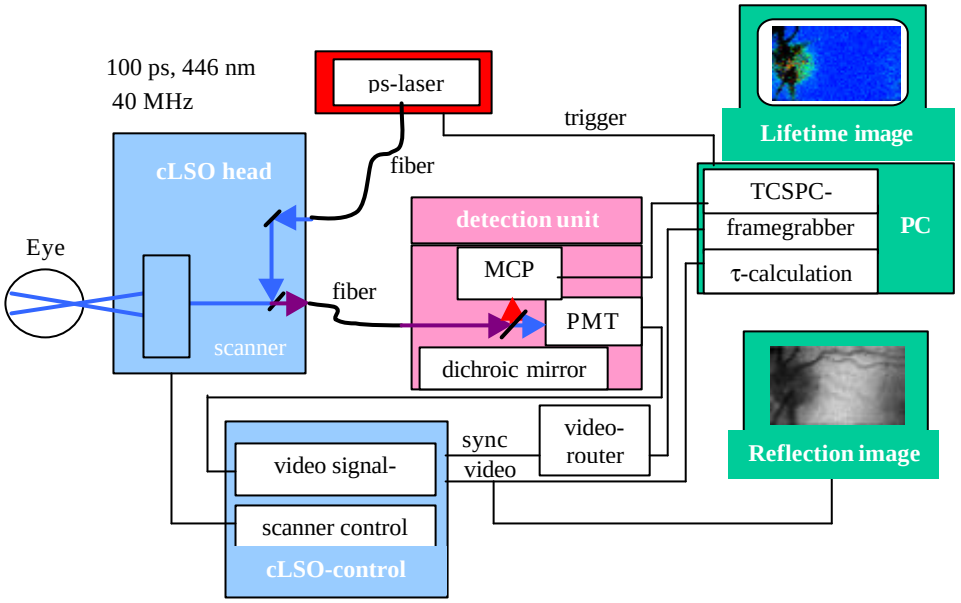

Fig. 1: Block diagram of the laser scanner ophthalmoscope for 2-dimensional lifetime measurement

The reflected light from the fundus and also the fluorescence light is confocally imaged onto a pinhole in the cLSO. Both parts of light are led to a separate detector unite by a 300 µm fibre. In the detector unite, a dichroic filter (DT blue, Linos, Goettingen, Germany) separates the fluorescence light from the reflected light, which is additionally blocked by a cut off filter (GG 475, Linos, Goettingen, Germany). The reflected light and the fluorescence light are detected simultaneously. The fluorescence light is detected by a micro-channel plate photo-multiplier MCP-PMT (HAM-R3809U-50, Hamamatsu, Herrsching, Germany), which is sensitive between 180 and 850 nm and has jitters < 50 ps. The reflected fundus light is detected by the original photo-multiplier of the cLSO and grabbed as reflection images by a frame grabber (INSPECTA- 4A, Mikrotron, Eching, Germany). For measurement of the 2 dimensional auto-fluorescence of the fundus in time – correlated single photon counting technique, the board SPC 730 (Becker/Hickl,

Berlin, Germany) is used. The router VRT – 1 (Becker/ Hickl, Berlin, Germany) synchronises the mechanical scanning process and the process on the SPC board. The measurement of the dynamic auto-fluorescence is controlled by a home build program.
The investigator aligns the ophthalmoscope in relation to the dilated pupil of patients eye until the region of interest appears in a 20° field as video reflection image with a sufficient contrast. The spatial pixel resolution in the time-resolved fluorescence images can be selected between 20 x 20 µm^2 and 160 x 160 µm^2. The time of 25 ns between 2 excitation pulses can be resolved in 64 up to 1024 time channels. So, a minimal time resolution of about 25 ps is possible. The memory on the SPC 730 board is limited to 8 MB. So, the selection of the highest spatial with the best time resolution results in a reduction of the size of the region of interest in the fluorescence image. An optimal combination is a spatial resolution of 80 x 80 µm^2 in combination with 1024 time channels for practical application. The measuring time can continuously be chosen between 40 ms and 3 s, depending on patients co-operation. If the eye is open for longer times, the tear film lacerates at the cornea, resulting in an increased light scattering and a weak pain. The patient is now blinking. During the measuring process, the patient hears an acoustical signal. After this measurement, the investigator sees both the reflection image of the fundus in a 20° field and the fluorescence image of the selected region of interest. The fluorescence signal of each pixel is the sum of photons in all time channels. The number of photons is colour-coded and the maximal value is given numerically. As for bi-exponential approximation of the fluorescence decay about 2000 photons should be collected per pixel, the investigator can decide, how often lifetime measurements should be repeated. The eye is a moving object and can fixate only for a certain time slot. So, the position of fluorescence images is changed at the fundus between single measurements. For registration of the fluorescence images, the simultaneously detected contrast - rich reflection images are used. The investigator excludes all inapplicable images and selects a reference image. After that, the registration of the reflection images occurs automatically[8]. As there is a fixed relation between the pixels in the reflection images and in the fluorescence images, the fluorescence images are registered in this way. During registration, the number of photons is accumulated in the corresponding time channels.

3. Evaluation of lifetime images

3.1 Measurement of 2-dimensional lifetime distribution

To investigate , whether changes after provocation of the metabolism are detectable by lifetime measurements, 2 tests were performed. The first was a provocation by breathing 100% oxygen. In this test, 3 measurements were taken. After a baseline measurement, the respiration of 100% oxygen started for 6 minutes. At this time, the second fluorescence image was detected. After that, the proband was breathing air for 15 minutes again and the third fluorescence image was taken.
In a second trial, the influence of dark adaptation on auto-fluorescence was studied. Again three measurements were performed: first a baseline image under room illumination, the second image after dark adaptation for about 3 minutes and the third image after receptor bleaching by looking in a 60 W lamp at a distance of 60 cm for about 15 s.
Furthermore, in first studies, lifetime images were taken from patients, suffering from exudative age-related macular degeneration. For comparison, images of the dynamic auto-fluorescence were measured from young healthy subjects in the same 20° field with the macula in the centre.
For interpretation of in vivo measurements, the dynamic auto-fluorescence was determined for some isolated substances under the same measuring conditions.

3.2 Evaluation by diagrams of lifetime distribution
3.2.1 Occurrence of the sum of tau 1 and tau 2

In earlier studies, a bi – exponential fit, according to equation (1) was found sufficient for approximation of dynamic auto - fluorescence of the eye – ground.

$$\frac{I(t)}{I_o} = a_1 \cdot e^{-\frac{t}{t_1}} + a_2 \cdot e^{-\frac{t}{t_2}} + b \quad with \quad a_i - amplitudes, \; t_i - lifetimes, \; b - offset \qquad (1)$$

Binning all pixels in the image or measuring in the oscilloscope mode results in one single fluorescence decay curve versus time. Such a curve has a high number of counts in all time channels and can be evaluated using the Fluofit

program (Picoquant, Berlin, Germany). In this kind of evaluation, local different lifetimes in fundus images stay undiscovered.
The SPCImage programs (Becker/ Hickl, Berlin, Germany) are now available for 2 – dimensional calculation of lifetime. In a first version, the sum of the occurrence of lifetimes tau 1 and tau 2 could be presented in a diagram. Such diagrams show, how often each lifetime was determined in the region of interest (ROI). Using this diagram, the optic disc and a range of the same size in the papillo – macular bundle were chosen as ROI. As shown in Fig. 2, considerable differences could be found in the occurrence of both lifetimes between these specific anatomical structures. If the ROI will be increased, the relative contribution of single locations is reduced in the entire lifetime distribution.

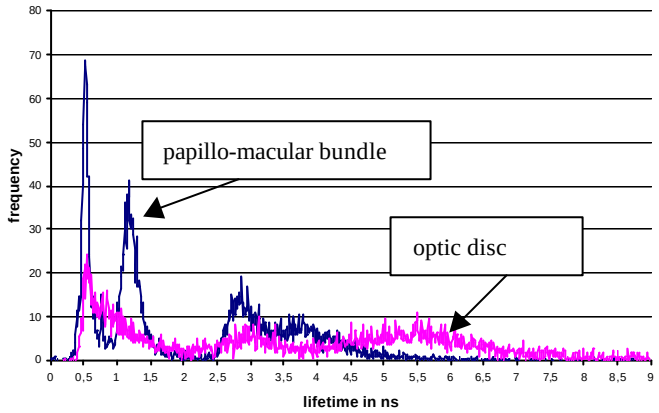

Fig. 2: Occurrence of lifetimes in the optic disc and in the papillo – macular bundle

The reproducibility of lifetime distributions was determined in the same ROI in the papillo – macular bundle in 3 fluorescence images, taken in a time distance of several weeks. As shown in Fig. 3, the curves cover each other quite good.

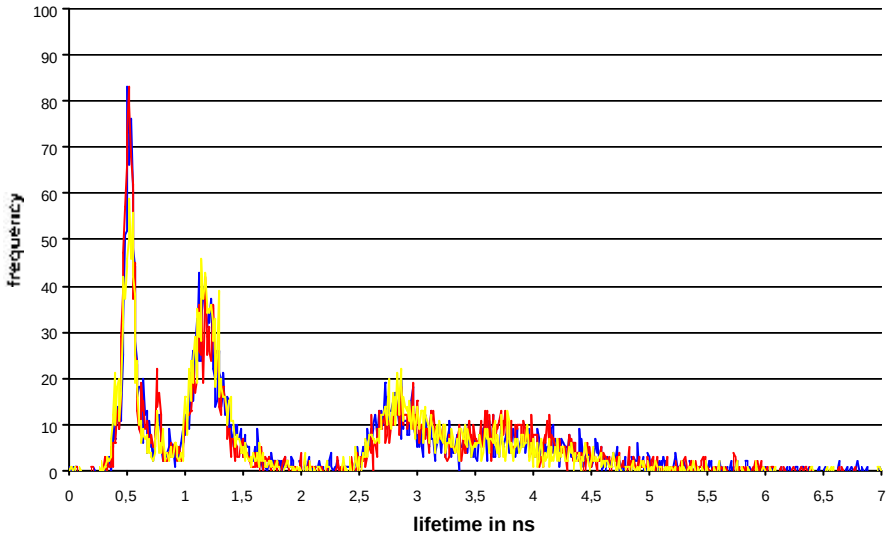

Fig. 3: Reproducibility of lifetime distribution in the papillo macular bundle. The lifetime distribution was calculated from the same region in 3 lifetime images taken in time distance of weeks.

As result of oxygen breathing, clear changes in the lifetime distribution could be found especially in the optic disc. As shown in Fig. 4, there are intervals of lifetime alterations around 0.6 ns where the occurrence decreases and around 3.4 ns where the occurrence of lifetime increases after oxygen breathing. In the papillo-macular bundle a decreased occurrence of lifetime was also found in the range of short lifetimes around 0.4 ns.

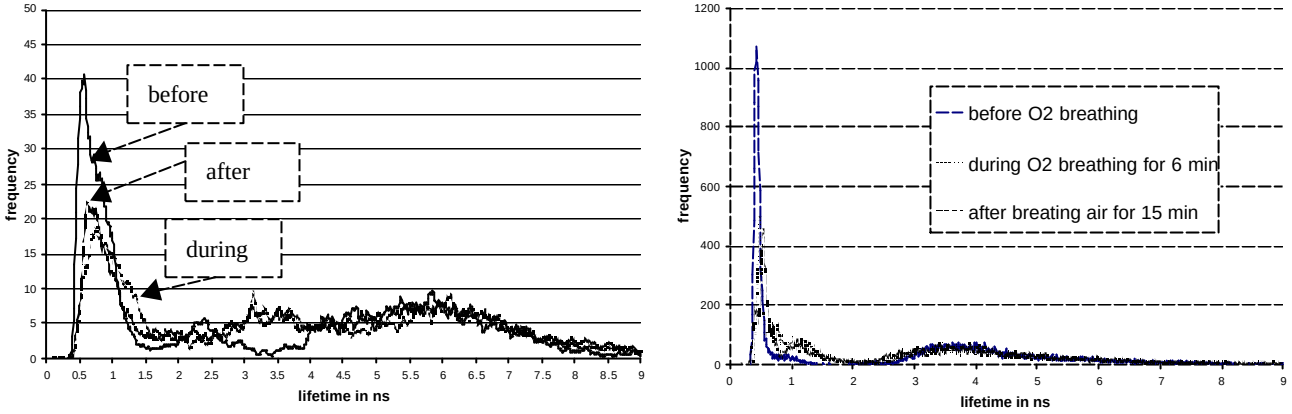

a) optic disc b) papillo-macular bundle

Fig. 4: Changes in occurrence of lifetime after oxygen breathing a) in the optic disc and b) in the papillo-macular bundle. Avoiding to much noise, the curves in the optic disc are calculated as moving average over 10 data points.

The measurement of changes in auto-fluorescence lifetime images as result of dark adaptation is difficult The eye under investigation must stay during dark adaptation exactly in the same position as during baseline measurement. Otherwise new adjustments under bright light would result in receptor bleaching. The 3 curves of occurrence of lifetime in the papillo-macular bundle under room light, during dark adaptation, and after bleaching are given in Fig. 5. In this diagram, the frequency of detected lifetimes around 0.5 ns is considerably increased during dark adaptation. The same behaviour was remarkable also for lifetimes around 4.4 ns. At 1.2 ns and 3 ns the occurrence of lifetime was decreased during dark adaptation.

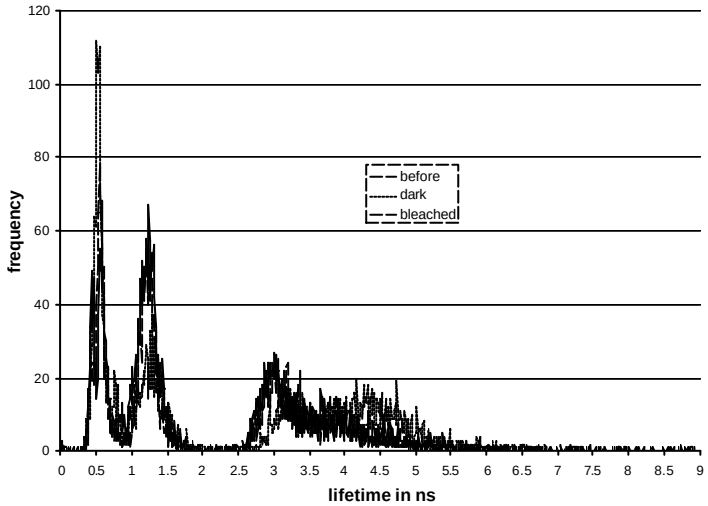

Fig. 5: Changes in occurrence of lifetime during dark adaptation and bleaching in the papillo-macular bundle.

3.2.2 Separate occurrence of tau 1 and of tau 2

More detailed information is available when the occurrence of lifetime can be separately investigated for tau 1 and for tau 2. That is possible applying version the program SPCImage 2.0 (Becker /Hickl, Berlin, Germany) and higher. If

only one fluorophor would act at the fundus, having a bi-exponential decay, the lifetime diagram would exhibit two narrow peaks, one in the tau 1 the other in the tau 2 diagram. The provocation of metabolism by respiration of oxygen was repeated in young subjects. Fig. 6 shows changes in the occurrence of tau 1 and of tau 2 in the macular region. The maximum of occurrence of tau 1 around 0.31 ns is altered to longer values and returned partly after respiration of air. In contrast, the distribution of tau 2 around 2.5 ns is changed to shorter lifetimes during oxygen breathing and only a limited part of longer lifetimes has reached the same frequency of occurrence after respiration of air as before oxygen breathing.

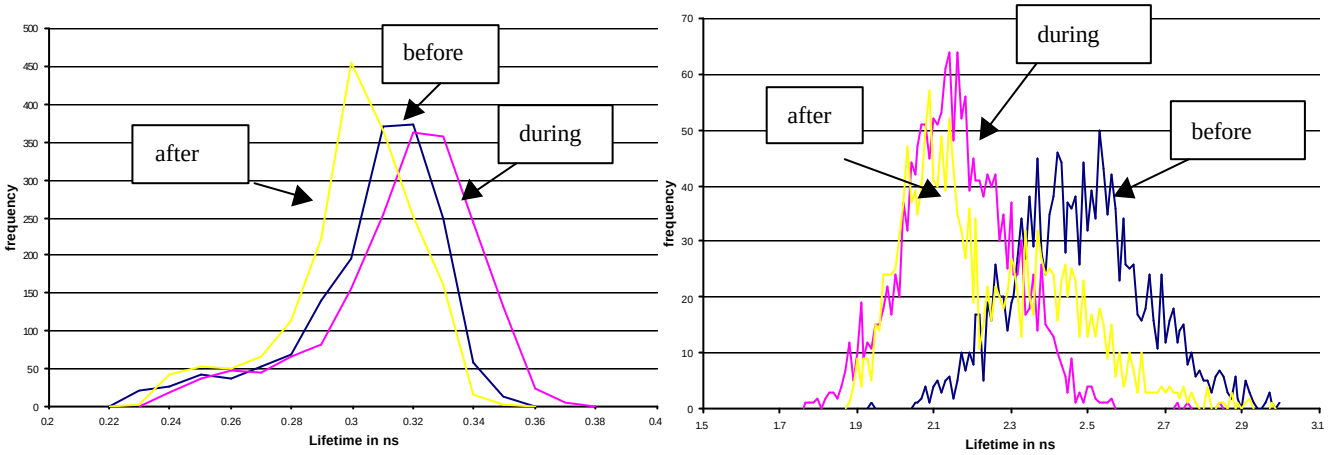

a) lifetime tau 1 b) lifetime tau 2

Fig. 6: Separate changes in occurrence of lifetime in the macular region before oxygen breathing, during oxygen breathing for 6 min. after breathing air for 15 min.. The distribution of occurrence of tau 1 is moved during oxygen breathing to longer values and is changed after respiration of air to shorter values as during baseline measurement. In contrast, the lifetime tau 2 is changed to shorter values during oxygen provocation and is moved partially back to the baseline measurement after breathing air.

3.2.3 Diagram tau 2 versus tau 1

During approximation of fluorescence decay versus time, a pair of lifetimes tau 1 and tau 2 is calculated for each pixel in the image. If all pairs of lifetimes are put in a diagram tau 2 versus tau 1, clusters of points, representing lifetime pairs of certain fluorophores can be identified. Now it is clear, that the diagrams of occurrence of tau 1 or of tau 2 are the projections of the lifetime clusters onto the corresponding lifetime axis. So, a limitation of diagrams of occurrence of lifetime is remarkable. If two lifetime clusters are in the same range of tau 1, but in different ranges of

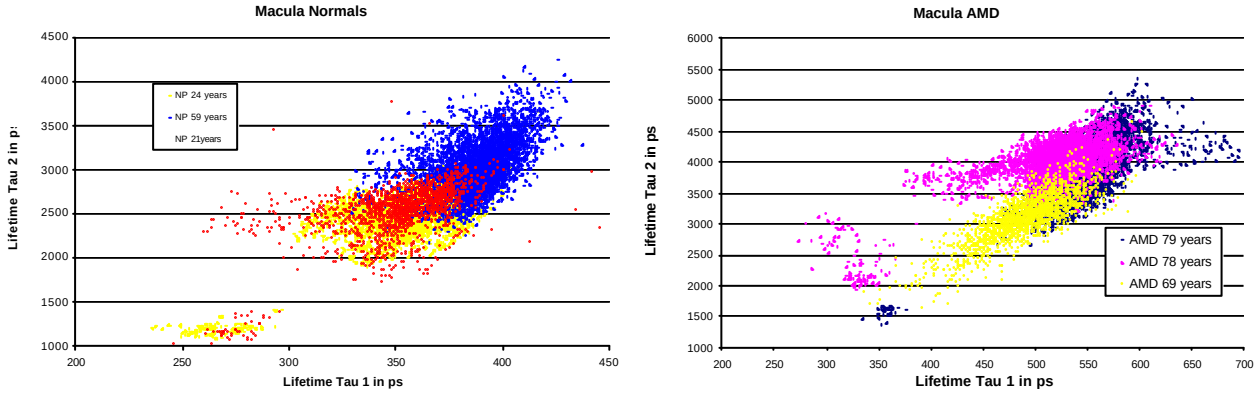

a) b)

Fig. 7: Lifetime diagram tau 2 versus tau 1 in the macula a) 3 normal subjects b) 3 exudative AMD-patients. The pathologic lifetime clusters in AMD are moved both for tau 1 and for tau 2 to longer values.

tau 2, in the diagram of occurrence of tau 1 the sum of the projection of both clusters is presented and no discrimination between both clusters is possible. As an example of the value of tau 1- tau 2 diagrams, the clusters of three lifetime measurements of normals in the age of 21, 24, and 59 years were compared with lifetime clusters of AMD patients in the age 69, 78, and 79 years (Fig. 7). All these measurements were performed in a 20° field with the macula in the centre.

From these diagrams follows a good discrimination between healthy subjects and patients, suffering from AMD. Another question is, which fluorophores are detectable in healthy or in pathologically altered eyes. Such a comparison is possible, measuring the dynamic auto-fluorescence of isolated substances in cuvettes. As the fluorescence lifetime depends on solvent, pH-value, temperature, viscosity, binding to proteins, or anisotropy, comparable conditions are required for in vitro and for in vivo measurements. If a substance exhibits a mono-exponential decay, two forms of lifetime clusters are possible. In the first kind of cluster, the lifetime pairs are centred around the same value for tau 1 and tau 2. In a second form, the extension of the cluster is narrow in one lifetime co-ordinate and is considerably extended in the second lifetime co-ordinate. That means, the surface of the lifetime profile has a sharp minimum for one lifetime, but the other lifetime has a flat minimum. The second lifetime has only a weak influence and can vary in an extended range. As an example, the lifetime clusters are shown in Fig. 8 for NADH (10 mM), FAD (10 mM), advanced glycation end-product (AGE, 0.75 mM) all dissolved in PBS. Additionally, the lifetime cluster of isolated granula of isolated human lipofuscin is drawn in Fig. 8. Lipofuscin is assumed to play an important role in development of AMD. This metabolic by-product consists of 10 components, according to Eldred and Katz[10]. Component 8 of lipofuscin was analysed as A2E by Sakai et al.[11] and synthesised by Eldred and Lasky[12], Parrish[13]. In this study, we used A2E, synthesised by Gaillard[14]. The lifetime cluster of A2E, non-physiologically dissolved in acetonitril, is also presented in Fig. 8.

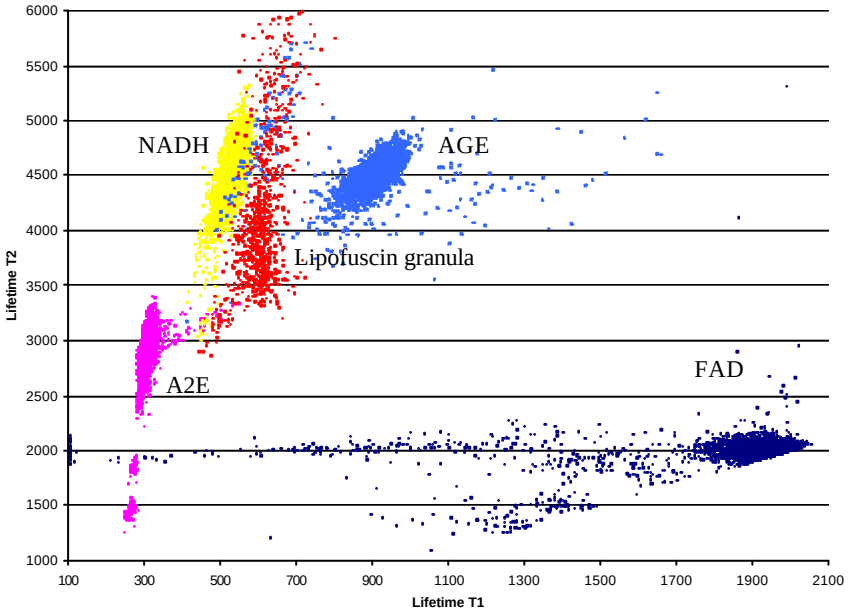

Fig.8: Lifetime clusters of isolated substances: NADH, FAD, AGE, A2E, and human lipofuscin.

3.2.4 Lifetime images

Clinical diagnoses in ophthalmology are done predominantly in fundus images. So, lifetime images, in which known anatomical structures like optic disc, macula, or the vessel system are present, are well suited as functional images. Again, two forms of presentation are possible: a continuously colour-coded range of lifetime tau 1 or of tau 2 or the presentation of selected lifetime ranges. In Fig. 10, the continuously change of tau 1 as response to oxygen respiration in the macula is demonstrated between 250 ps and 350 ps. In accordance to the diagram of occurrence of lifetime in Fig. 7, the contribution of longer lifetimes is reduced during oxygen breathing. After respiration of air for 15 minutes, the contribution of longer lifetimes is increased again.

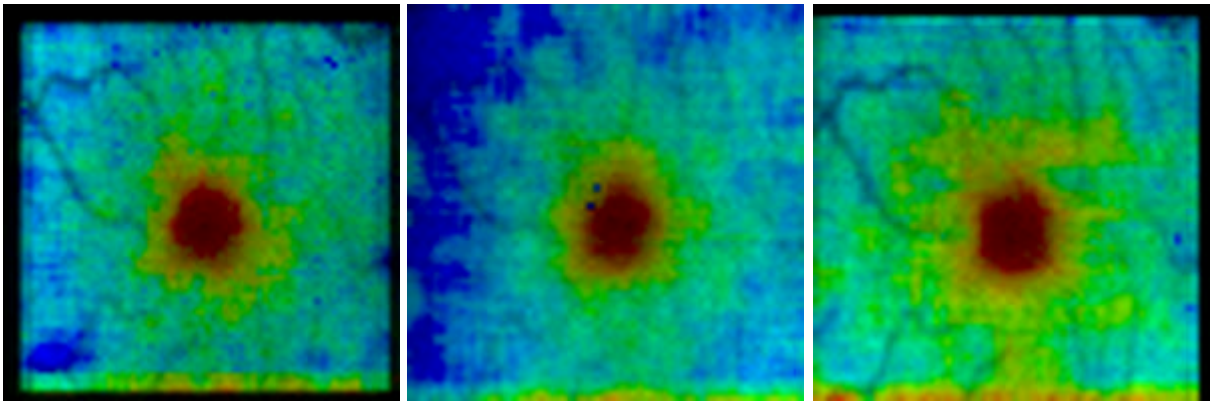

Fig. 9: Continuously alteration of lifetime tau 1 in the macula after oxygen breathing. a) baseline image, b) after breathing oxygen for 6 minutes, c) after respiration of air for 15 minutes. The lifetime range is between 250 ps and 350 ps. During oxygen breathing, the contribution of longer tau 1 values is increased. Caused by the oxygenation of blood, the capillaries appear in a weak contrast.

The investigation of lifetime in selected intervals is also informative. If it is known, in which interval of lifetime certain substances fluoresces, a change of the local appearances of fluorescence in this interval of time can be determined after provocation test. Such an example is given in Fig. 11. In the first line of this figure, all pixels are given, exhibiting a lifetime in the range between 0.35 ns up to 0.62 ns. In the first image, nearly all pixels outside the optic disc fluoresces in this lifetime range before oxygen provocation. After respiration of 100% oxygen for 6 minutes, a considerable lower number of pixels fluoresces. As shown in the second line, a reverse behaviour is remarkable in the lifetime range between 0.7 ns and 1.2 ns. Before oxygen provocation, only the optic disc fluoresces in this range, but after oxygen respiration also a considerable number of pixels outside the optic disc exhibit a fluorescence in this lifetime interval.

4. Discussion

Lifetime measurements can be performed by the laser scanning lifetime ophthalmoscope both on subjects and on cuvettes. The registration of time-resolved fluorescence images corresponding to the registration of parallel detected reflection images realises an accumulation of a sufficient number of photons in all time channels. Though, a bi-exponential approximation of the fluorescence decay versus time can be realised with an acceptable uncertainty. Increasing the photon number by binning of pixels results in a further reduction of uncertainty in the determination of lifetime, but local deviation of lifetime are no more detectable.

In case of cataract, the excitation light at 446 nm is considerably attenuated and the reflection image has only a weak contrast. This problem can be solved, when laser diodes are available, emitting optimally at 470 nm.

Several programs can now be used for the 2-dimensional calculation of lifetime. Some improvements are possible according to the special task of industrial tests. Assuming, the lifetime is independent of the excitation or emission range, a global fit should considerably improve the uncertainty of lifetime calculation. When the lifetimes are determined for all fundus pixels, there are different methods for evaluation the results. The calculation of diagrams of occurrence of lifetime in selected ROI allows a first interpretation. A better comparison between in vivo measurements in different ROI both in normals and in patients is possible by drawing lifetime clusters in diagrams of tau 2 versus tau 1. So, the correspondence can considerably improved between results of in vivo measurements and results, determined on isolated substances. This tool is not realised in industrial solutions until now

Most important for clinical application are images of fluorescence lifetime. Here, the detection of local deviations of lifetime with a high contrast is necessary. First functional defects might be determined after provocation tests. For this task, the investigation of the fundus in selected intervals of lifetime might be promising.

The decreased frequency of lifetime during oxygen breathing in the lifetime interval around 0.5 ns in Fig. 4 and the reduction of fluorescent pixels in the lifetime range between 0.35nm and 0.63 nm after oxygen respiration points to the detection of changes in the equilibrium of NAD-NADH. The oxidised form NAD, which should be increased during oxygen breathing, is less fluorescent than the reduced form NADH. The increased occurrence of fluorescence in this

short interval of lifetime during dark adaptation can be explained by an increased metabolic activity. The activated metabolism leads to a relative loss of oxygen, resulting an in creased contribution of NADH in the equilibrium of the

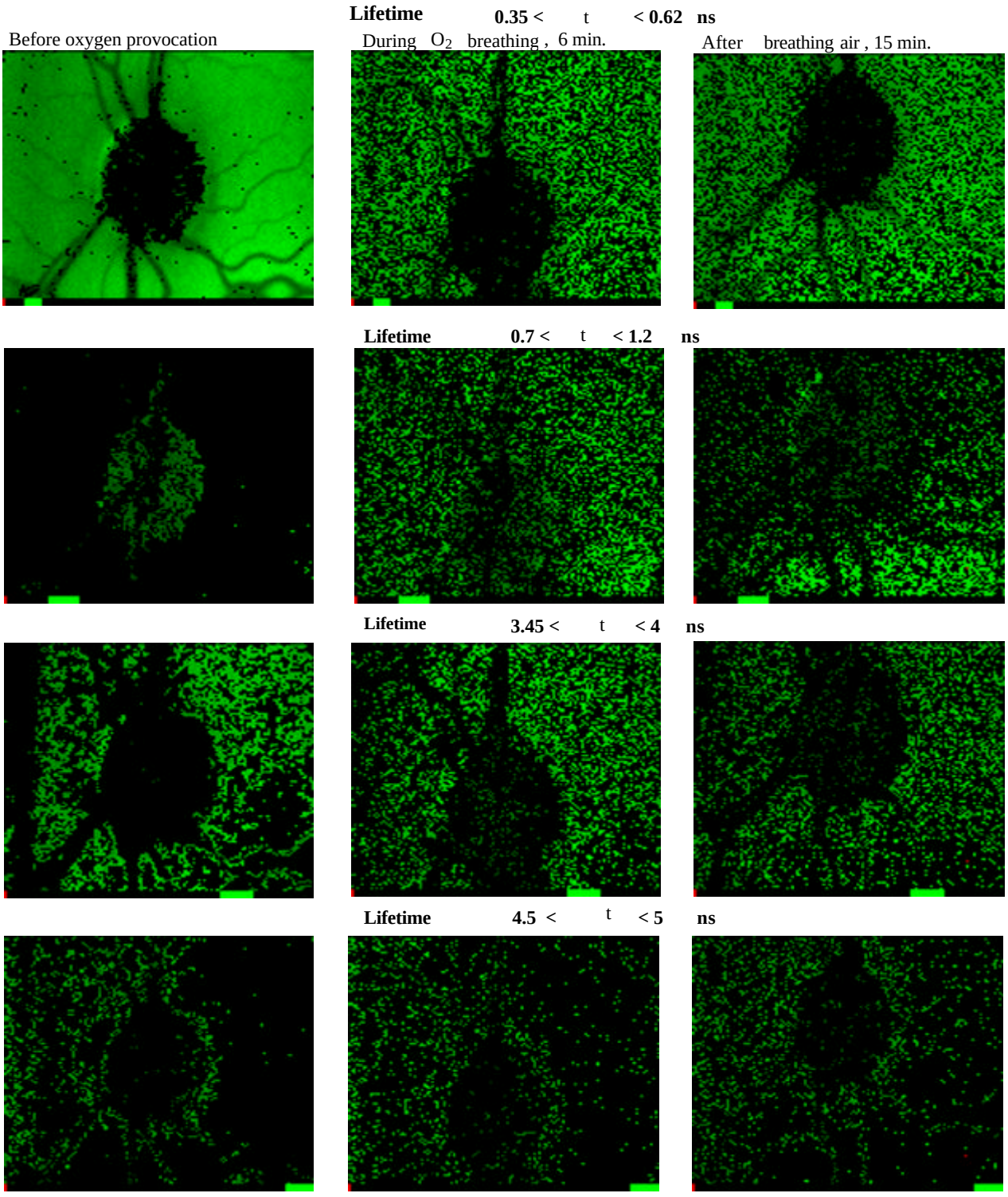

Fig. 11: Alteration of fluorescence in selected lifetime ranges after respiration of 100% oxygen.

redox pair NAD-NADH. This assumption is supported by Cringle[15], who found a reduction of the partial pressure of oxygen during dark adaptation in the retina of rat.

5. Summary

As shown by these examples, provoked changes in the metabolism seems to be measurable by time-resolved auto-fluorescence of the human ocular fundus. It is assumed that early alterations occur in the metabolism of cells before manifest pathologic signs are detectable by known ophthalmologic methods. Such pre-pathologic alterations might be found by time-resolved auto-fluorescence. Applying an equivalent therapy, the pathologic alterations might be reversible.

Acknowledgement

This research was supported by the Thuringiam Ministry of Science, Research , and Art A 309-00015. The authors are grateful to Dr. Sybille Franke, Department of Internal Medicine , University of Jena for providing advanced glycation end-products.

References:

1. Chance B "Pyridine nucleotide as an indicator of the oxygen requirements for energy-linked functions of mitochondria".Circ.Res. May; 38(5 Suppl 1): I31-8, 1976
2. Anderson-Engels A, Gustafson A, Johannson J, Stenram U, Svanberg K, Svanberg S "Investigation of Possible Fluorophores in Human Atherosclerotic Plaque" Laser in Life Science 5 (1-2): 1-11, 1992
3. Lakowicz, J. R. "Principles of Fluorescence Spectroscopy" Kluwer Academic/Plenum Publishers: New York, Boston, Dondrecht, London, Moscow, 1999
4. American National Standard for Use of Lasers ANSI Z 136.1-2000 (2000) Laser Institute of America, Suite 128, 13501 Ingenuite Drive, Orlando, FL 32826
5. Schweitzer D, Kolb A, Hammer M, Thamm E "Basic investigations for 2-dimensional time resolved fluorescence measurements at the fundus" International Ophthalmology 23: 4-6:399-404, 2001
6. Schweitzer D, Kolb A, Hammer M, Thamm E "Tau mapping of the autofluorescence of the human ocular fundus" Progress in biomedical optics and imaging, Vol. 1 No. 35 ISSN 1605-7422, Proceedings of SPIE, Vol. 4164, pp. 79-89
7. Schweitzer D, Kolb A, Hammer M "Autofluorescence lifetime measurements in images of the human ocular fundus" Progress in biomedical optics and imaging, Vol. 2 No. 32 ISSN 1605-7422, Proceedings of SPIE, Vol. 4432, pp. 29-39
8. Schweitzer D, Kolb A, Hammer M Anders R "Zeitaufgelöste Messung der Autofluoreszenz- ein Werkzeug zur Erfassung von Stoffwechselvorgängen am Augenhintergrund" Ophthalmologe 2002, Vol. 99, pp. 776-779
9. Voss K, Ortmann W, Suesse H "Bildmatching und Bewegungskompensation bei Fundus-Bildern" Proc. 20.DAGM-Symposium, Stuttgart 1998, "Mustererkennung 1998", Springer 1998, 439-446, also available under http://pandora.inf.uni-jena.de/papers/fundus/fundus.html
10. Eldred GE, Katz MR "Fluorophores of the Human Retinal Pigment Epithelium: Separation and Spectral Characterisation" Exp. Eye Res. 47, 71-86, 1988
11. Sakai N, Decatur J, Nakanishi K, Elderd GE "Ocular Age Pigment A2E: An Unprecedented Pyridinium Bisretinoid" J. Am. Chem. Soc. 118, 1559-1560, 1996
12. Eldred EG, Lasky MR "Retinal age pigments generated by self-assembling lysosomotropic detergents" Nature Vol. 361, 25 Feb. 724-726, 1993
13. Parish, C. A., Hashimoto, M., Nakanishi, K., Dillon, J., Sparrow, J. Isolation and one step preparation of A2E and iso A2E fluorophores from human retinal pigment epithelium. Proc Natl Acad Sci USA 95, 14609- 14613, 1998
14. Gaillard ER, Atherton SJ, Eldred GE, Dillon J " Photophysical Studies on Human Retinal Lipofuscin" Photochem. Photobiol. 61, 448-453, 1995
15. Cringle, St. J., Yu, D. Y., Yu, P. K., Su, E. N. "Intraretinal Oxygen Consumption in Rat in Vivo" Invest Ophthalmol Vis Sci 43, 6, 1922-1927, 2002